INTENSITY-HUE-SATURATION COLOUR DISPLAY TRANSFORM FOR HYPERSPECTRAL DATA*

Mario Beauchemin and Ko B. Fung
Canada Centre for Remote Sensing,
588 Booth Street, Ottawa, Canada, K1A 0Y7

ABSTRACT

A technique for producing consistent colour composites from hyperspectral data is presented. It is based on the intensity-hue-saturation (IHS) colour transform, a model related to the human perception of colours. The method is simple and robust. The ordinary moment (order zero) of the spectral distribution is assigned to the Intensity component - the perceived luminance. The center of gravity of the distribution is used for the Hue component - the dominant wavelength or colour. Finally, the fraction of the total flux (Intensity) inside a window of a predefined width centered at the Hue (center of gravity) is taken as the Saturation - the purity of the dominant wavelength. A saturation measure derived from variance is also considered, providing a full moment-based IHS transform. Each component is linearly stretched for contrast enhancement and projected to the RGB colour space using the hexcone model. The method is illustrated with a *casi* (Compact Airborne Spectrographic Imager) image. Further tests are needed to evaluate the potentials of the method for diversified landscapes and different sensor configurations.

1.0 INTRODUCTION

Colour products are one of the effective media used in remote sensing to display information. How to use colour and its shades to present dominant and embedded information in a multiple band image is a major issue for photointerpretation. Sensors are now available with an increasing number of spectral bands and the display of the information content of such datasets is a major challenge. A good sampling of existing visualization techniques for hyperspectral data can be found in Staenz *et al*. (1998). There are two common approaches to display hyperspectral data through the RGB system in 2-D. The first one is to perform a judicious choice of a 3-band subset. The selection can be based on *a priori* knowledge of spectral properties, or based on statistical methods (*e.g*. Sheffield, 1985; Chavez *et al*.,1982). A second approach consists in performing dimension reduction. The principal component (PC) analysis is certainly the most widely used approach for such a purpose. Each approach has its advantages and disadvantages. Band selection methods maintain the data integrity but the amount of information is

* Presented at the Fourth International Airborne Remote Sensing Conference and Exhibition/
21st Canadian Symposium on Remote Sensing, Ottawa, Ontario, Canada, 21-24 June 1999.

limited to that contained in the selected bands. The PC approach takes advantage of the statistics of the whole dataset but the results are highly scene-dependant. It gives rise to colour composites that are sometimes difficult to interpret (*e. g*., vivid colours), and it does not preserve the data integrity (Harris *et al*., 1990).

In this paper, a simple and robust method for synoptic visualization of information encapsulated in hyperspectral data is presented. It consists of characterizing the global spectral distribution attributes to fit the intensity-hue-saturation (IHS) frame. The method has been tested on a small dataset and the results are compared with those derived from principal components.

2.0 METHOD

The IHS colour transform has been widely used to display information in remote sensing (*e. g*., references cited in Harris *et al*., 1990; Pohl and Van Genderen, 1998). A major strength of the IHS technique is the fact that this approach is related to the human perception of colours (Foley *et al*., 1990). The hue corresponds to the dominant wavelength of the light seen, the saturation is the proportion of pure light of the dominant wavelength, and the intensity represents the amount of light. This is a functional definition and, thus, can be adapted to spectral distributions of arbitrary spectral range. In the following, we employ the general label 'object' for the physical entity that gives rise to the measured spectral distribution. For clarity, the sampling rate in the wavelength domain is assumed constant so that the band number replaces the wavelength value in the formulae. However, all expressions can be easily extended to the general case of arbitrary sampling (*e.g*., Rundquist and Di 1989).

Among many possibilities, the intensity of an object in an image can be charaterized by the maximum value of the spectral distribution or by a measure that integrates the corresponding signal in each band. To have greater immunity against noise and bad pixel values, the latter case is chosen for our algorithm development. For a N-band spectral distribution, we define the intensity-related measure y of an object by:

$$y = \sum_{k=1}^{N} DN_k \, , \tag{1}$$

where DN_k is the pixel digital number DN value in band k, k=1,…, N. Normalization of equation (1) by N ($y_N = y / N$) results in the expression for the moment of order zero, or ordinary moment (Rundquist and Di, 1989). The centre of gravity (CG) of a distribution is statistically close to its mean wavelength and, therefore, is a good candidate for the hue. It is given by:

$$CG = \sum_{k=1}^{N} k\, DN_k \Big/ \sum_{k=1}^{N} DN_k \, . \tag{2}$$

This is referred to as the mean by Rundquist and Di (1989). It is equivalent to the ratio of the moment of order one to the moment of order zero. Finally, any parameter that describes how the distribution peaks around the hue can be used to measure the saturation level. The square root of the variance is obviously one such measure and can be derived from moment analysis. The normalized variance (μ_2) of order 2 (Staenz 1996) is given by:

$$\mu_2 = \frac{1}{N} \sum_{k=1}^{N} [(k - CG)^2 DN_k \Big/ \frac{1}{N} \sum_{k=1}^{N} DN_k \, . \tag{3}$$

The signal inside a small set of bands centred at hue, divided by the signal in the entire spectra, represents another intuitive and simple measure for saturation (f):

$$f = \frac{1}{N} \sum_{k=CG-w/2}^{CG+w/2} DN_k \Big/ \frac{1}{N} \sum_{k=1}^{N} DN_k \, , \tag{4}$$

where w is a range of bands. The IHS transform is fully moment driven and parameter-free if based on equations (1), (2) and (3).

The hexacone model is employed to transform the IHS components to the RGB system (Foley *et al*., 1990). Input data for that model are scaled according to $0<i<1$, $0<s<1$ and $0<h<360$, where i, s, and h are the intensity, saturation and hue variables respectively (see figure 13.34 of Foley *et al*., 1990). Hereafter, we will denote the resulting output channels as r, g, b. An important property of the IHS system is that each component can be manipulated independently (Gillepsie *et al*., 1986). To enhance visual contrast, a linear stretch is applied prior to the IHS to the RGB transform. The final transformations adopted in this work are:

$$i = (y_N - y_{N\,\mathrm{min}}) / (y_{N\,\mathrm{max}} - y_{N\,\mathrm{min}}), \tag{5}$$

$$h = (2/3)\, 360\, [\, 1 - (CG - CG_{\mathrm{min}}) / (CG_{\mathrm{max}} - CG_{\mathrm{min}})\,], \tag{6}$$

$$s_f = (f - f_{\min}) / (f_{\max} - f_{\min}), \text{ and} \tag{7a}$$

$$s_{\mu 2} = [\, 1 - (\sqrt{\mu_2} - \sqrt{\mu_2}_{\ \min}) / (\sqrt{\mu_2}_{\ \max} - \sqrt{\mu_2}_{\ \min}) \,], \tag{7b}$$

where the *min* and *max* indicate histogram bounds. In the present work, they correspond to plus or minus 2.4 standard deviations from the average value calculated for each component. The hue equation (6) is inverted and rescaled to fit two-third of the hexacone model range. This is done to avoid the magenta colour in the RGB system. This inversion and rescaling process is esthetical in essence but permit to match, in an intuitive manner, the human perception of colour. Effectively, as the dominant wavelength of the objects varies from one extreme to the other, that is from shorter to longer wavelengths, so it is for its displayed colours (blue to red). Scale inversion is also performed for equation (7b) because the variance behaves in a reciprocal way with saturation: the lower is the variance and the higher is the saturation, and conversely. No such inversion is needed for equation (7a).

3.0 PROCEDURES

A 256 x 256 pixels region of 24 bands has been extracted from a 72-band *casi* image cube acquired in Labrador on July, 1996. The pixel size is 5 meters and the centre wavelength ranges from 414 nm to 953 nm, in step of about 23 nm. Although the sampling interval has a minor effect, it has nevertheless been taken into account for the hue calculation (wavelength instead of band number domain). The *DN*s are proportional to the radiance. The landscape is mainly composed of wood (hard/soft/mixed), water, wetlands, rocks and lichen (mainly in open forests). The sampling interval was assumed constant for the intensity and saturation calculation. The first three principal components were also derived to establish a baseline for comparison. Conditions imposed by the software used for the PC analysis limits the number of bands to less than 32. One band out of every three bands was selected from the original 72-band cube for a total of 24 selected bands. Equations (5), (6) and (7) were applied on this 24 bands subset. The first three principal components represent 76.5, 19.8 and 2 per cent of the total variance, respectively.

4.0 RESULT AND DISCUSSION

The i, h, and s_f components are displayed in Figure 1, along with the first three principal components ($PC1$, $PC2$, $PC3$). Each image has been linearly stretched. Expression (7a) was used for the saturation. This measure depends on a free parameter, w, that defines the set of bands centred at hue. A too small number of bands in the set will give rise to a measure sensitive to noise effects. A too large number of bands will make the measure insensitive to saturation effects. We choose a set with the number of bands equals to a fifth of the spectral range (w=5 bands). Although there were differences between the images produced by equations (7a) and (7b), they nevertheless generate very small visual differences when projected into the RGB space. Visually, there are many similarities between the two sets of images shown in Figure 1. The i and $PC1$ images in Figures 1a and 1b look very much the same, this is supported by the high value of the correlation coefficient, $r_{i,PC1}$=0.98. Although the values of the h component have been inverted, its overall similarity with $PC2$ is also striking ($r_{h,PC2}$ = -0.82)(Figures 1c and d). The s and $PC3$ components in Figures 1e and f are poorly correlated ($r_{s,PC3}$ = - 0.16) and look dissimilar. The saturation s is moderately correlated with the hue h, with $r_{s,h}$ = 0.78; it drops to 0.58 if s is given by equation (7b). Note that i and h are weakly correlated, $r_{i,h}$ = 0.32. By design, no correlation exists between any pair of the principal components. This comparison is not aimed at establishing a relationship between principal components and i, h and s. Only a correlation between the intensity and the first principal component is somehow expected since the major source of variation in a scene corresponds to object brightness most of the time.

We found that, overall, the IHS to RGB colour transform compares well visually to a RGB composite made from the first three principal components with $PC1$ in red, $PC2$ in green and $PC3$ in blue (not shown). This reflects the high level of correlation between i and $PC1$, h and $PC2$, and the fact that $PC1$ and $PC2$ represent 96.3 per cent of the total variance. However, as expected, the attributed colours for the same landform differ by a wide margin. Another (expected) difference is the intensity effect that generates a dark colour for low-radiance objects, *e. g.*, water, which shows up in colour in the PC composite. We found that the RGB composite based on PC may provide better colour contrast between some landforms. For example, wetlands appear yellow while the surrounding is blue (mainly forest). In the case of the RGB composite based on the IHS technique, the wetland areas are bright light green compared to a dark green colour for the surrounding area. However, by adjusting the origin of the hue, comparable high colour contrasts are obtained for the IHS-based RGB composite. This operation is equivalent to re-directing the generated r, g, b channels to a different combination of colour guns, *e.g.*, r in blue, g in red and b in green. Note that such a hue manipulation completely cancels out the 'esthetical' effect introduced in equation (6) but the colour coding is still consistent.

Essentially, the proposed method relies on the first three moments of the distributions. Rundquist and Di (1989) have shown that moment analysis applied on imaging spectrometer data is a useful technique for data reduction. Staenz (1996) also demonstrated that, overall, band reduction by moment analysis performs well for classification purposes. These results have linkage to the fact that, theoretically and under certain conditions, moments determine completely a distribution (Stuart and Ord, 1994). In this study, we used a few moments and as a result only the overall spectral information is characterized. In the Staenz (1996) study, the normalized concentrated moment apparently possesses higher discriminant power than CG (eq. 6). However, the coefficient of correlation between CG and the normalized concentrated moment in our dataset is 0.986, indicating a very high level of redundancy between the two measures. It is possible that improved results could be obtained by replacing the variance used for the saturation variable by a higher order moment.

5.0 CONCLUSIONS

An IHS-based method has been introduced to display the global characteristics of spectral distributions. The method is simple and robust. A small area that include different landforms such as forest, water, wetlands, rocks and lichen has been used to assess the potential of the method from a 24-band image. A comparison with the first three principal components that account for about 98 per cent of the total variance, reveals the usefulness of the method proposed.

We like to stress that PC analysis is able to pick-up fine details while the *i, h, s* remains a technique designed to catch the overall characteristics of a distribution (it is restricted to a few moments of a distribution). The results presented here are preliminary and have been tested on a very small test area. Further tests are needed to evaluate the full potential of the method for diversified landscapes as well as for different sensor configurations (*e. g*., wavelength range).

6.0 REFERENCES

P. S. Chavez, G. L. Berlin, and L. B. Sowers, "Statistical methods for Selecting Landsat MSS Ratios," *Journal of Applied Photographic Engineering*. Vol. 8, No. 1, pp. 23-30, 1982.

J. D. Foley, A. Dam, S. K. Feiner, and J. F. Hughes, In *Computer Graphics Principles and Practice*, eds. Addison-Wesley, Reading, Chap. 13, p. 593. 1990.

A. B. Gillespie, A. B. Kahle, and R. E. Walker, "Colour Enhancement of Highly Correlated Images I. Decorrelation and HIS Contrast Stretches," *Remote Sensing of Environment*. Vol. 20, pp. 209-235, 1986.

J. R. Harris, R. Murray, and T. Hirose, "IHS Transform for the Integration of Radar Imagery with other Remotely Sensed Data." *Photogrammetric Engineering and Remote Sensing*, Vol. 56, No. 12, pp. 1631-1641, 1990

C. Pohl, and J. L. Van Genderen, "Multisensor Image Fusion in Remote Sensing: Concepts, Methods and Applications," *International Journal of Remote Sensing*. Vol. 19, No. 5, pp. 823-854, 1998.

D. C. Rundquist, and L. Di, "Band-Moment Analysis of Imaging-Spectrometer Data," *Photogrammetric Engineering and Remote Sensing*, Vol. 55, No. 2, pp. 203-208, 1989.

C. Sheffield, "Selecting Band Combinations from Multispectral Data," *Photogrammetric Engineering and Remote Sensing*, Vol. 51, No. 6, pp. 681-687, 1985.

K. Staenz, "Classification of a Hyperspectral Agricultural Data Set Using Band Moments for Reduction of the Spectral Dimensionality," *Canadian Journal of Remote Sensing*, Vol. 22, No. 3, pp. 248-257, 1996.

K. Staenz, "ISDAS - A System for Processing/Analysing Hyperspectral Data," *Canadian Journal of Remote Sensing*, Vol. 24, No. 2, pp. 99-113, 1998.

A. Stuart, and K. J. Ord, In *Kendall's Advanced Theory of Statistics, Volume 1, Distribution theory*, eds. John Wiley & Sons Inc., New York, Chap. 3, p.111, 1994.

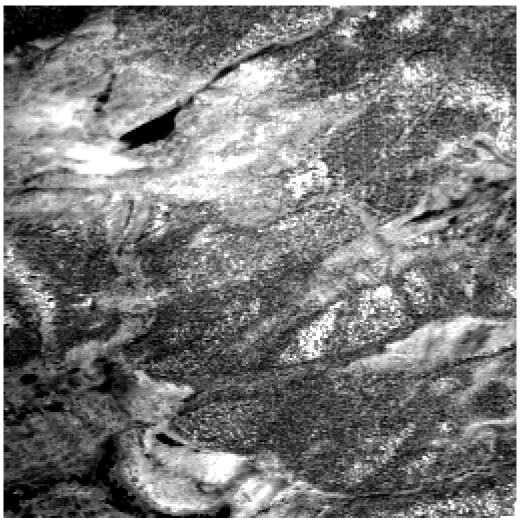

Figure 1a. Intensity Image

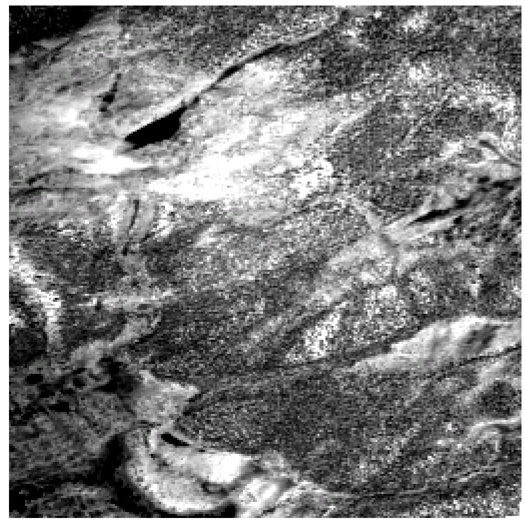

Figure 1b. PC1 Image

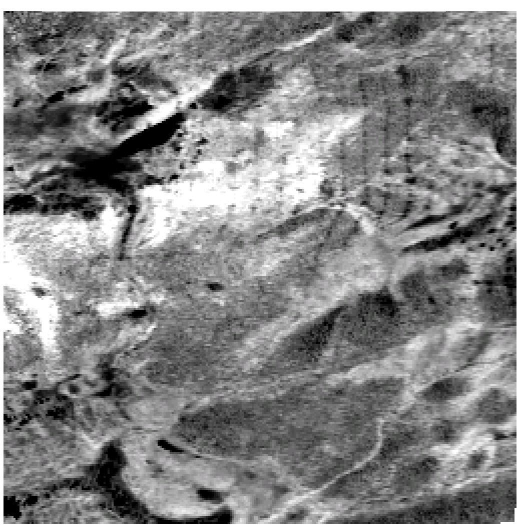

Figure 1c. Hue Image

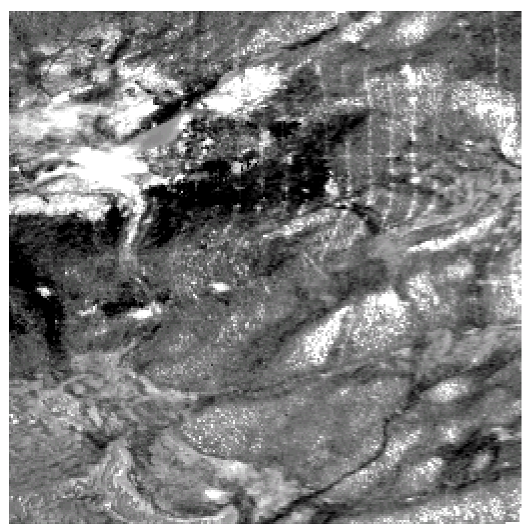

Figure 1d. PC2 Image

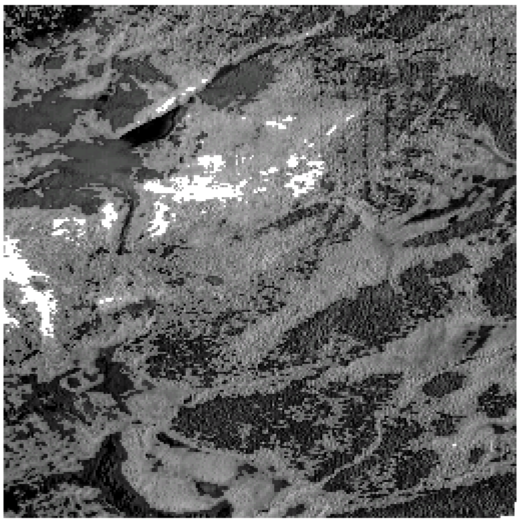

Figure 1e. Saturation Image

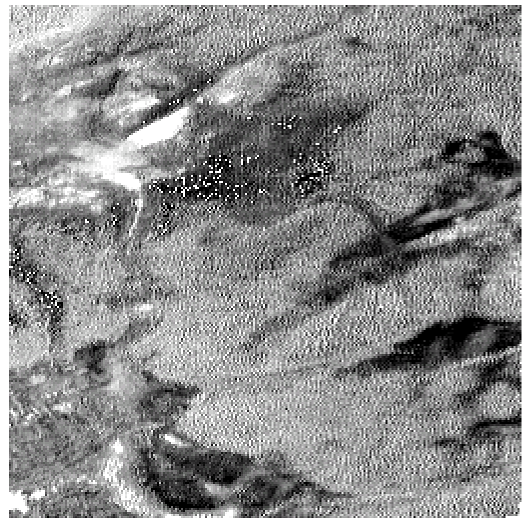

Figure 1f. PC3 Image

Figure 1. Intensity, Hue, and Saturation Images (1a, 1c, 1e) and Principal Component Images: PC1, PC2 and PC3 (1b, 1d, 1f).